ASYMPTOTICALLY EXACT A *POSTERIORI* ERROR ESTIMATES FOR THE LOCAL DISCONTINUOUS GALERKIN METHOD FOR NONLINEAR KDV EQUATIONS IN ONE SPACE DIMENSION

MAHBOUB BACCOUCH

Abstract. In this paper, we develop and analyze an implicit *a posteriori* error estimates for the local discontinuous Galerkin (LDG) method for nonlinear third-order Korteweg-de Vries (KdV) equations in one space dimension. First, we show that the LDG error on each element can be split into two parts. The first part is proportional to the $(p+1)$-degree right Radau polynomial and the second part converges with order $p + \frac{3}{2}$ in the L^2-norm, when piecewise polynomials of degree at most p are used. These results allow us to construct *a posteriori* LDG error estimates. The proposed error estimates are computationally simple and are obtained by solving a local steady problem with no boundary conditions on each element. Furthermore, we prove that, for smooth solutions, these *a posteriori* error estimates converge at a fixed time to the exact spatial errors in the L^2-norm under mesh refinement. The order of convergence is proved to be $p + \frac{3}{2}$. Finally, we prove that the global effectivity index converges to unity at $\mathcal{O}(h^{\frac{1}{2}})$ rate. Several numerical examples are provided to illustrate the global superconvergence results and the convergence of the proposed error estimator.

Key words. Local discontinuous Galerkin method, nonlinear KdV equations, superconvergence, *a posteriori* error estimation.

1. Introduction

KdV-type equations describe the propagation of waves in a variety of nonlinear, dispersive media and appear often in many physical applications; see *e.g.* [27, 30] and the references therein. In this paper, we propose and analyze a residual-based *a posteriori* error estimator for the local discontinuous Galerkin (LDG) method for one-dimensional nonlinear Korteweg-de Vries (KdV) equations of the form

$$(1a) \quad u_t + (f(u))_x + u_{xxx} = g(x,t), \quad x \in \Omega = [a,b], \ t \in [0,T],$$

subject to the initial condition

$$(1b) \qquad\qquad u(x,0) = u_0(x), \quad x \in [a,b],$$

and periodic boundary conditions. Here, $g(x,t)$, and $u_0(x)$ are some given smooth functions. We assume that the nonlinear flux function $f(u)$ is sufficiently smooth with respect to the variable u and the exact solution is also smooth on $[a,b] \times [0,T]$ for a fixed time T. For the sake of simplicity,

we only consider periodic boundary conditions. This assumption is not essential and the LDG scheme can be easily designed for purely Dirichlet or Mixed Dirichlet-Neumann boundary conditions; see [4, 7, 13, 19] for some discussion.

The LDG method is a successful numerical technique for solving linear and nonlinear partial differential equations (PDEs) containing higher than first-order spatial derivatives. It was first introduced by Cockburn and Shu [29] for solving convection-diffusion problems. Since then, several LDG schemes have been developed and analyzed for various high order differential equations in one and multiple dimensions including two-point boundary-value problems [20, 21, 22, 23, 24], convection-diffusion problems [2, 4, 7, 13, 26, 29], second-order wave equations [3, 9, 10, 11, 14], the sine-Gordon equation [15, 16, 17, 18, 25], KdV-type equations [12, 19, 31, 33, 34, 35, 36, 37], and the fourth-order Euler-Bernoulli beam equation [5, 6, 8], just to mention a few. The LDG method has many advantages over the classical numerical methods available in the literature such as the finite difference and finite element methods. For instance, LDG methods are robust and high-order accurate, can achieve stability without slope limiters, and are element-wise conservative. Moreover, LDG methods are extremely flexible in the mesh-design, they can easily handle meshes with hanging nodes, elements of various types and shapes, and local spaces of different orders. As we shall see below, they further exhibit global superconvergence properties that can be used to construct asymptotically exact *a posteriori* error estimates by solving a local residual problem on each element. More details about the LDG methods for high order time dependent PDEs can be found in the review paper [35] and the proceeding of Shu [32]. Furthermore, some LDG methods for solving high order PDEs were developed by Yan and Shu [38], which were high order accurate and stable schemes.

In [12], we presented *a posteriori* error estimates for the LDG method for the linearized KdV equation in one space dimension $u_t + \alpha u_x + \beta u_{xxx} = 0$. The proposed error estimates are computationally simple and are obtained by solving a local steady problem with no boundary condition on each element. We proved that the significant parts of the spatial discretization errors for the LDG solution and its spatial derivatives (up to second order) are proportional to $(p+1)$-degree Radau polynomials. We used these results to develop asymptotically exact *a posteriori* error estimates. We also proved that, for smooth solutions, the proposed *a posteriori* LDG error estimates for the solution and its spatial derivatives, at a fixed time t, converge to the true errors at $\mathcal{O}(h^{p+\frac{3}{2}})$ rate. The purpose of this paper is to extend these results to nonlinear KdV equations of the form (1). In [19], we presented and analyzed a superconvergent LDG scheme for solving (1). Optimal *a priori* error estimates for the LDG solution and for the two auxiliary variables that approximate the first- and second-order derivatives are derived in the L^2-norm. The order of convergence is proved to be $p + 1$. We also proved that the derivative of the LDG solution is superconvergent with order $p + 1$

towards the derivative of a special projection of the exact solution. Finally, we proved that the LDG solution is superconvergent with order $p + \frac{3}{2}$ toward a special Gauss-Radau projection of the exact solution. Our proofs are valid for arbitrary regular meshes using P^p polynomials with $p \geq 1$ and under the condition that $|f'(u)|$ possesses a uniform positive lower bound.

In this paper, we present and analyze an implicit *a posteriori* LDG error estimate for the nonlinear KdV equation (1). We use the results of the first part of this work [19] to prove that the significant part of the spatial discretization error for the LDG solution is proportional to the $(p + 1)$-degree right Radau polynomial, when piecewise polynomials of degree at most p are used. We use this result to construct a residual-based *a posteriori* error estimate for the spatial error. The leading term of the discretization error is estimated by solving a local steady problem with no boundary conditions on each element. We further prove that the proposed LDG error estimate converges to the true spatial error at $\mathcal{O}(h^{p + \frac{3}{2}})$ rate. Finally, we prove that the global effectivity index in the L^2-norm converges to unity at $\mathcal{O}(h^{\frac{1}{2}})$ rate. In our analysis we proved these convergence results under mesh refinement and at a fixed time t and time discretization is assumed to be exact. Our proofs are valid for any regular meshes and using piecewise polynomials of degree $p \geq 1$. We would like to point out that the present LDG method has several features over the standard numerical methods due to the following nice properties: (i) the LDG method can be easily designed for any order of accuracy (the order of accuracy can be locally determined in each cell, thus allowing for efficient p-adaptivity), (ii) it can be used on arbitrary triangulations, even those with hanging nodes, thus allowing for efficient h-adaptivity, (iii) the LDG method provides optimal convergence properties for both the solution and the auxiliary variables that approximate its derivatives, (iv) the LDG method is extremely local in data communications (the evolution of the solution in each cell needs to communicate only with the immediate neighbors, regardless of the order of accuracy, thus allowing for efficient parallel implementations), and (iv) it achieves superconvergence properties, which play a key role to construct asymptotically exact *a posteriori* error estimators.

The rest of the paper is organized as follows: In section 2 we present the semi-discrete LDG method for solving the nonlinear KdV equation (1). We also recall some preliminary results from the first part of this work [19], which will be needed in our error analysis. In section 3 we prove the main superconvergence result towards the p-degree right Radau interpolating polynomial. This result will be used to prove that the LDG error can be split into a significant part, which is proportional to the $(p + 1)$-degree right Radau polynomial, and a less significant part, which converges to zero in the L^2-norm at $\mathcal{O}(h^{p + \frac{3}{2}})$ rate. In section 4 we present and analyze our *a posteriori* error estimation procedure. In section 5 we present numerical results to illustrate the global superconvergence results and the convergence

of the proposed error estimator. We conclude and discuss our results in section 6.

2. The LDG scheme and preliminary results

2.1. The LDG scheme. Here, we recall the LDG scheme for solving (1) [19]. The main idea of the LDG method is to rewrite (1) into a system of first-order PDEs and then discretize it by the standard DG method. To do this, we introduce two auxiliary variables $q = u_x$ and $r = q_x$ to convert (1a) into the first-order system

$$(2) \qquad u_t + (f(u))_x + r_x = g, \qquad r - q_x = 0, \qquad q - u_x = 0.$$

Next, we subdivide the domain $\Omega = [a, b]$ into N intervals $I_i = [x_{i-1}, x_i]$, $i = 1, 2, \ldots, N$, where $a = x_0 < x_1 < \cdots < x_N = b$. The length of I_i is denoted by $h_i = x_i - x_{i-1}$. Let $h = \max\limits_{1 \le i \le N} h_i$ be the length of the largest interval. In our analysis, we assume that the mesh is quasi-regular in the sense that the ratio between the maximum and the minimum mesh sizes stays bounded during mesh refinements.

Let $v\big|_i$ be the value of the continuous function v at $x = x_i$. For simplicity, we use $v^-\big|_i$ and $v^+\big|_i$ to denote the left limit and the right limit of v at the discontinuity point x_i, i.e.,

$$v^-\big|_i = v(x_i^-, t) = \lim_{s \to 0^-} v(x_i + s, t), \qquad v^+\big|_i = v(x_i^+, t) = \lim_{s \to 0^+} v(x_i + s, t).$$

Multiplying the three equations in (2) by three different test functions v, w, and z, respectively, integrating over the interval I_i, and using integration by parts, we get

(3a)
$$\int_{I_i} u_t v \, dx - \int_{I_i} (r + f(u)) v_x \, dx + (f(u) + r) v\big|_i - (f(u) + r) v\big|_{i-1} = \int_{I_i} g v \, dx,$$

(3b)
$$\int_{I_i} r w \, dx + \int_{I_i} q w_x \, dx - q w\big|_i + q w\big|_{i-1} = 0,$$

(3c)
$$\int_{I_i} q z \, dx + \int_{I_i} u z_x \, dx - u z\big|_i + u z\big|_{i-1} = 0.$$

We define the following discontinuous finite element space

$$V_h^p = \{v : v|_{I_i} \in P^p(I_i), \ i = 1, 2, \ldots, N\},$$

where $P^p(I_i)$ is the space of polynomials of degree at most p on I_i with coefficients as functions of t.

The LDG scheme consists of finding u_h, q_h, $r_h \in V_h^p$, such that, $\forall\, v$, w, $z \in V_h^p$ and $\forall\, i = 1, 2, \ldots, N$,

$$\int_{I_i} (u_h)_t v\, dx - \int_{I_i} (r_h + f(u_h)) v_x\, dx$$

(4a)
$$+(\hat{f} + \hat{r}_h) v^- \big|_i - (\hat{f} + \hat{r}_h) v^+ \big|_{i-1} = \int_{I_i} g v\, dx,$$

(4b)
$$\int_{I_i} r_h w\, dx + \int_{I_i} q_h w_x\, dx - \hat{q}_h w^- \big|_i + \hat{q}_h w^+ \big|_{i-1} = 0,$$

(4c)
$$\int_{I_i} q_h z\, dx + \int_{I_i} u_h z_x\, dx - \hat{u}_h z^- \big|_i + \hat{u}_h z^+ \big|_{i-1} = 0,$$

where $\hat{f}$, $\hat{u}_h$, $\hat{q}_h$, and $\hat{r}_h$ are the so-called numerical fluxes, which are, respectively, the discrete approximations to $f(u)$, u, q, and r at the nodes. In this paper, we take the following numerical fluxes [19]:

- The numerical flux $\hat{f}$ associated with the convection is taken as the Godunov flux *i.e.*, for $i = 0, 1, \ldots, N$,

(4d)
$$\hat{f}\big|_i = \hat{f}(u_h(x_i^-, t), u_h(x_i^+, t)) = \begin{cases} \displaystyle\min_{u_h^- \leq u \leq u_h^+} f(u), & \text{if } u_h^- < u_h^+, \\ \displaystyle\max_{u_h^+ \leq u \leq u_h^-} f(u), & \text{if } u_h^- \geq u_h^+. \end{cases}$$

- The numerical fluxes $\hat{u}_h$, $\hat{q}_h$, and $\hat{r}_h$ can be taken as

(4e)
$$\hat{u}_h\big|_i = u_h^- \big|_i, \qquad \hat{q}_h\big|_i = q_h^+ \big|_i, \qquad \hat{r}_h\big|_i = r_h^+ \big|_i, \qquad i = 0, 1, \ldots, N.$$

To complete the definition of the LDG scheme, we still need to define the discrete initial condition $u_h(x, 0) \in V_h^p$. In this paper, we use a special projection $\mathbb{P}_h$ of the exact initial condition $u_0(x)$

(5)
$$u_h(x, 0) = \mathbb{P}_h u(x, 0), \ x \in I_i, \ i = 1, 2, \ldots, N.$$

The projection $\mathbb{P}_h$ is needed to prove global superconvergence result toward Gauss-Radau projections; see [19]. It is defined as follows: Suppose q_h, $r_h \in V_h^p$ are the unique solutions (with given $\mathbb{P}_h u$) to

(6a)
$$\int_{I_i} r_h w\, dx + \int_{I_i} q_h w_x\, dx - q_h^+ w^- \big|_i + q_h^+ w^+ \big|_{i-1} = 0, \quad \forall\, w \in V_h^p,$$

(6b)
$$\int_{I_i} q_h z\, dx + \int_{I_i} \mathbb{P}_h u\, z_x\, dx - (\mathbb{P}_h u)^- z^- \big|_i + (\mathbb{P}_h u)^- z^+ \big|_{i-1} = 0, \quad \forall\, z \in V_h^p,$$

then we require

(7a)
$$(P_h^- u - \mathbb{P}_h u)^- \big|_i = (P_h^+ q - q_h)^+ \big|_i - (P_h^+ r - r_h)^+ \big|_i,$$

(7b)
$$\int_{I_i} (P_h^- u - \mathbb{P}_h u) v\, dx = \int_{I_i} \left((P_h^+ q - q_h) - (P_h^+ r - r_h) \right) v\, dx, \quad \forall\, v \in P^{p-1}(I_i),$$

where $q = u_x$, $r = q_x$, and $P_h^{\pm} u$ are two Gauss-Radau projections of u onto V_h^p defined element-by-element by the following conditions

(8a) $\quad \int_{I_i} (P_h^- u - u) v dx = 0, \ \forall \ v \in P^{p-1}(I_i), \quad \text{and} \quad (P_h^- u - u)^-\big|_i = 0,$

(8b) $\quad \int_{I_i} (P_h^+ u - u) v dx = 0, \ \forall \ v \in P^{p-1}(I_i), \quad \text{and} \quad (P_h^+ u - u)^+\big|_{i-1} = 0.$

As discussed in [19, 31], $\mathbb{P}_h$ is only needed for technical purposes in the proof of superconvergence results. In our numerical examples we used the projection P_h^- and observed similar conclusions.

2.2. Preliminary results. In this subsection, we recall some results from [19] which will be needed in our error analysis. First, we introduce some notation and definitions. The L^2-norm of $u(x,t)$ over I_i is denoted by $\|u\|_{0,I_i} = \left(\int_{I_i} u^2(x,t) dx \right)^{\frac{1}{2}}$. Let $H^s(I_i)$, $s = 0, 1, \ldots$ be the standard Sobolev space

$$H^s(I_i) = \left\{ u \ : \ \int_{I_i} |\partial_x^k u(x,t)|^2 dx < \infty, \ 0 \le k \le s \right\}.$$

The $H^s(I_i)$-norm is defined as

$$\|u\|_{s,I_i} = \left(\sum_{k=0}^{s} \left\| \partial_x^k u(\cdot,t) \right\|_{0,I_i}^2 \right)^{\frac{1}{2}}.$$

The norm on the whole computational domain Ω is defined as

$$\|u\|_{s,\Omega} = \left(\sum_{i=1}^{N} \|u\|_{s,I_i}^2 \right)^{\frac{1}{2}}.$$

We remark that if $u \in H^s(\Omega)$, then $\|u\|_{s,\Omega}$ is the standard Sobolev norm $\left(\sum_{k=0}^{s} \left\| \partial_x^k u \right\|_{0,\Omega}^2 \right)^{\frac{1}{2}}$.

For simplicity, we use $\|u\|$ and $\|u\|_s$ to denote $\|u\|_{0,\Omega}$ and $\|u\|_{s,\Omega}$, respectively. Finally, use $\|u(0)\|$ to denote $\|u(\cdot, t = 0)\|$.

Let $e_u = u - u_h$, $e_q = q - q_h$ and $e_r = r - r_h$ denote the errors between the exact solutions of (2) and the LDG solutions defined in (4). We note that the actual errors can be decomposed into two parts as

(9) $\qquad\qquad e_u = \epsilon_u + \bar{e}_u, \quad e_q = \epsilon_q + \bar{e}_q, \quad e_r = \epsilon_r + \bar{e}_r,$

where $\epsilon_u = u - P_h^- u$, $\epsilon_q = q - P_h^+ q$ and $\epsilon_r = r - P_h^+ r$ are the projection errors and $\bar{e}_u = P_h^- u - u_h$, $\bar{e}_q = P_h^+ q - q_h$ and $\bar{e}_r = P_h^+ r - r_h$ are the errors between the LDG solutions and the projection of the exact solutions.

Throughout the paper, the letter C (with or without subscript) will denote a generic positive constant that is independent of the mesh size h, but it may depend upon the exact smooth solution u of (1a). Note that C is not necessarily the same at each occurrence.

Now, we are ready to state several error estimates from [19]. These estimates will be needed in our error analysis.

Theorem 2.1. *Let $p \geq 1$. Let $(u, q = u_x, r = q_x)$ and (u_h, q_h, r_h) be the exact and LDG solutions of (2) and (4), where $u_h(x, 0)$ is defined in (5). We assume that $u \in H^{p+3}(\Omega)$ and $u_t \in H^{p+1}(\Omega)$. Also, we assume that the flux function $f(u) \in C_b^3(\mathbb{R})$, where $C_b^m(D)$ is the set of real m-times continuously differentiable functions which are bounded together with their derivatives up to the mth order. Then, there exists a positive constant C independent of h such that, $\forall \, t \in [0, T]$,*

$$\text{(10a)} \qquad \|e_u\| + \|e_q\| + \|(e_u)_t\| + \|e_r\| \;\leq\; Ch^{p+1},$$

$$\text{(10b)} \qquad \|(\bar{e}_u)_x\| \;\leq\; Ch^{p+1},$$

$$\text{(10c)} \qquad \|\bar{e}_u\| \;\leq\; Ch^{p+\frac{3}{2}}.$$

Proof. All proofs can be found in [19]. More precisely, the estimate (10a) can be found in its Theorem 3.1. The superconvergence result (10b) can be found in its Theorem 4.1. Finally, the estimate (10c) is given in its Theorem 4.4. □

3. Superconvergence towards the right Radau interpolating polynomial

In this section, we prove an important superconvergence result towards the p-degree right Radau interpolating polynomial. This result will be used to prove that the LDG error e_u can be split into a significant part, which is proportional to the $(p + 1)$-degree right Radau polynomial, and a less significant part, which converges to zero in the L^2-norm at $\mathcal{O}(h^{p+\frac{3}{2}})$ rate.

Before we state the main superconvergence result, we need some properties of the Legendre of Radau polynomials. Let $\tilde{L}_p(\xi)$ be the Legendre polynomial of degree p on the reference interval $[-1, 1]$. It can be defined by the Rodrigues formula [1]

$$\text{(11a)} \qquad \tilde{L}_p(\xi) = \frac{1}{2^p p!} \frac{d^p}{d\xi^p} \left((\xi^2 - 1)^p \right), \quad -1 \leq \xi \leq 1.$$

The Legendre polynomial satisfies the properties $\tilde{L}_p(1) = 1$, $\tilde{L}_p(-1) = (-1)^p$, and the orthogonality relation

$$\text{(11b)} \qquad \int_{-1}^{1} \tilde{L}_p(\xi) \tilde{L}_q(\xi) d\xi = \frac{2}{2p+1} \delta_{pq},$$

where δ_{pq} is the Kronecker symbol.

From (11a), we can easily deduce that

$$\tilde{L}_{p+1}(\xi) = \frac{(2p+2)!}{2^{p+1}[(p+1)!]^2} \xi^{p+1} + \tilde{q}_p(\xi), \quad \text{where } \tilde{q}_p \in P^p([-1, 1]),$$

which gives

$$(11c) \qquad \tilde{L}_{p+1}^{(p+1)}(\xi) = \frac{(2p+2)!}{2^{p+1}(p+1)!}.$$

The $(p+1)$-degree right Radau polynomial on $[-1,1]$ is defined by

$$(11d) \qquad \tilde{R}_{p+1}(\xi) = \tilde{L}_{p+1}(\xi) - \tilde{L}_p(\xi), \quad -1 \leq \xi \leq 1.$$

We note that $\tilde{R}_{p+1}(\xi)$ has $p+1$ real distinct roots $-1 < \xi_0 < \cdots < \xi_p = 1$.

Mapping the physical element I_i into the reference element $[-1,1]$ by the standard affine mapping

$$(11e) \qquad x = \frac{x_i + x_{i-1}}{2} + \frac{h_i}{2}\xi,$$

we get the p-degree shifted Legendre and right Radau polynomials on I_i

$$L_{p,i}(x) = \tilde{L}_p\left(\frac{2x - x_i - x_{i-1}}{h_i}\right), \quad R_{p,i}(x) = \tilde{R}_p\left(\frac{2x - x_i - x_{i-1}}{h_i}\right), \quad x \in I_i.$$

Using the mapping (11e) and the orthogonality relation (11b), we obtain

$$(11f) \quad \|L_{p,i}\|_{0,I_i}^2 = \int_{I_i} L_{p,i}^2(x)dx = \frac{h_i}{2}\int_{-1}^1 \tilde{L}_p^2(\xi)d\xi = \frac{h_i}{2}\frac{2}{2p+1} = \frac{h_i}{2p+1}.$$

Throughout this paper the roots of $R_{p+1,i}(x)$, $x \in I_i$ are denoted by

$$(11g) \qquad x_{i,j} = \frac{x_i + x_{i-1}}{2} + \frac{h_i}{2}\xi_j, \quad j = 0, 1, \ldots, p.$$

We note that the $(p+1)$-degree right Radau polynomial on I_i can be written as

$$(11h) \qquad R_{p+1,i}(x) = \frac{(2p+2)!}{h_i^{p+1}[(p+1)!]^2} \prod_{j=0}^{p}(x - x_{i,j}).$$

In the next lemma, we prove some properties of $R_{p+1,i}$ which will be needed in our *a posteriori* error analysis.

Lemma 3.1. *The $(p+1)$-degree right Radau polynomial on I_i satisfies the following properties*

$$(12) \qquad \|R_{p+1,i}\|_{0,I_i}^2 = c_p h_i, \quad \text{where } c_p = \frac{4(p+1)}{(2p+1)(2p+3)},$$

$$(13) \qquad \int_{I_i} R'_{p+1,i} L_{p,i} dx = 2.$$

Proof. In order to prove (12), we use the orthogonality relation (11b) to write

$$
\begin{aligned}
\|R_{p+1,i}\|_{0,I_i}^2 &= \int_{I_i} R_{p+1,i}^2(x)dx \\
&= \frac{h_i}{2}\int_{-1}^{1}\tilde{R}_{p+1}^2(\xi)d\xi \\
&= \frac{h_i}{2}\int_{-1}^{1}\left(\tilde{L}_{p+1}(\xi) - \tilde{L}_p(\xi)\right)^2 d\xi \\
&= \frac{h_i}{2}\int_{-1}^{1}(\tilde{L}_{p+1}^2(\xi) + \tilde{L}_p^2(\xi) - 2\tilde{L}_{p+1}(\xi)\tilde{L}_p(\xi))d\xi \\
&= \frac{h_i}{2}\left[\frac{2}{2p+3} + \frac{2}{2p+1}\right] \\
&= \frac{4(p+1)}{(2p+1)(2p+3)}h_i = c_p h_i,
\end{aligned}
$$

where $c_p = \frac{4(p+1)}{(2p+1)(2p+3)}$.

Next, we show (13). Using the definition of $R_{p+1,i}$ and the orthogonality relation (11b), we get

$$
\int_{I_i} R'_{p+1,i}L_{p,i}dx = \int_{I_i}\left(L'_{p+1,i} - L'_{p,i}\right)L_{p,i}dx = \int_{I_i} L'_{p+1,i}L_{p,i}dx,
$$

since $L'_{p,i}$ is a polynomial of degree $p-1$ on I_i.

Using integration by parts and the orthogonality relation (11b), we obtain

$$
\begin{aligned}
&\int_{I_i} R'_{p+1,i}L_{p,i}dx \\
&= L_{p+1,i}(x_i)L_{p,i}(x_i) - L_{p+1,i}(x_{i-1})L_{p,i}(x_{i-1}) - \int_{I_i} L_{p+1,i}L'_{p,i}dx \\
&= L_{p+1,i}(x_i)L_{p,i}(x_i) - L_{p+1,i}(x_{i-1})L_{p,i}(x_{i-1}).
\end{aligned}
$$

Since $L_{p+1,i}(x_i) = L_{p,i}(x_i) = 1$, $L_{p,i}(x_{i-1}) = (-1)^p$, and $L_{p+1,i}(x_{i-1}) = (-1)^{p+1}$, we have

$$
\int_{I_i} R'_{p+1,i}L_{p,i}dx = (1)(1) - (-1)^{p+1}(-1)^p = 2,
$$

which completes the proof of the lemma. $\square$

Next, we define two interpolating polynomials πu and $\hat{\pi}u$ as follows:

(1) The interpolating polynomial πu is defined element-by-element as follows: For any function u, $\pi u\big|_{I_i} \in P^p(I_i)$ and interpolates u at $x_{i,j}, j = 0, 1, \ldots, p$ (the $p+1$ roots of $R_{p+1,i}$).

(2) The interpolating polynomial $\hat{\pi}u$ is also defined element-by-element as follows: For any function u, $\hat{\pi}u\big|_{I_i} \in P^{p+1}(I_i)$ and interpolates

u at $x_{i,j}, j = 0, 1, \ldots, p$, and at an additional point $\bar{x}_i$ in I_i with $\bar{x}_i \neq x_{i,j}, j = 0, 1, \ldots, p$.

Remark 3.1. The operator $\hat{\pi}$ is needed for technical reasons in the proof of the error estimates. We would like to mention that the interpolating polynomial $\hat{\pi}u$ depends on the additional point $\bar{x}_i$. For clarity of presentation, we simply choose $\bar{x}_i = x_{i-1}$ (left-end point of I_i). We note that $\bar{x}_i \neq x_{i,j}, j = 0, 1, \ldots, p$. Moreover, we can easily verify the following

$$(14) \qquad \hat{\pi}u = \pi u + c_i(t) R_{p+1,i}(x),$$

since both $R_{p+1,i}(x)$ vanish at the Radau points $x_{i,k},\ k = 0, 1, \ldots, p$. Using (14) and the fact that $\hat{\pi}u(x_{i-1}, t) = u(x_{i-1}, t)$, we find

$$c_i(t) = \frac{u(x_{i-1}, t) - \pi u(x_{i-1}, t)}{R_{p+1,i}(x_{i-1})}.$$

We note that

$$R_{p+1,i}(x_{i-1}) = L_{p+1,i}(x_{i-1}) - L_{p,i}(x_{i-1}) = (-1)^{p+1} - (-1)^p = 2(-1)^{p+1} \neq 0.$$

In the next lemma, we state and prove some properties of P_h^- and π, which play important roles in our *a posteriori* error analysis. In particular, we prove that the interpolation error $u - \pi u$ can be divided into a significant and a less significant parts.

Lemma 3.2. *Let P_h^- and π be the Gauss-Radau and interpolating operators. Then*

$$(15) \qquad \pi v = P_h^- v, \quad \forall\, v \in P^{p+1}(I_i).$$

Moreover, if $u \in H^{p+2}(I_i)$, $t \in [0, T]$ fixed, then the interpolation error $u - \pi u$ can be split as:

$$(16) \qquad u - \pi u = \phi_i + \gamma_i, \quad \phi_i = \alpha_i(t) R_{p+1,i}(x), \quad \gamma_i = u - \hat{\pi}u, \quad on\ I_i,$$

where $\alpha_i(t)$ is the coefficient of $L_{p+1,i}$ in the $(p+1)$-degree polynomial $\hat{\pi}u$ and

$$(17a) \qquad \|\phi_i\|_{k,I_i} \ \leq \ Ch_i^{p+1-k} \|u\|_{p+1,I_i}, \quad 0 \leq k \leq p,$$

$$(17b) \qquad \|\gamma_i\|_{k,I_i} \ \leq \ Ch_i^{p+2-k} \|u\|_{p+2,I_i}, \quad 0 \leq k \leq p+1.$$

Finally, we have the following superconvergence result

$$(18) \qquad \left\| \pi u - P_h^- u \right\|_{0,I_i} \leq Ch_i^{p+2} \|u\|_{p+2,I_i}.$$

Proof. First we show (15). Let $v \in P^{p+1}(I_i)$. Then v can be split as $v(x) = v_1(x) + d_{p+1} L_{p+1,i}(x)$, where $v_1 \in P^p(I_i)$ and d_{p+1} is a constant. Applying the operators π and P_h^- and using the fact that $\pi v_1 = P_h^- v_1 = v_1,\ \forall\, v_1 \in P^p(I_i)$, we get

$$\pi v = v_1 + d_{p+1} \pi(L_{p+1,i}), \qquad P_h^- v = v_1 + d_{p+1} P_h^- (L_{p+1,i}).$$

Thus,
(19)
$$v - \pi v = d_{p+1} \left(L_{p+1,i} - \pi(L_{p+1,i}) \right), \quad v - P_h^- v = d_{p+1} \left(L_{p+1,i} - P_h^- (L_{p+1,i}) \right).$$

Using the standard interpolation error formula, the chain rule, (11c), and (11h), there exists $y \in I_i$ such that the interpolation error $L_{p+1,i} - \pi(L_{p+1,i})$ is

$$L_{p+1,i} - \pi(L_{p+1,i}) = \frac{L_{p+1,i}^{(p+1)}(y)}{(p+1)!} \prod_{j=0}^{p} (x - x_{i,j})$$

$$= \frac{(2p+2)!}{h_i^{p+1}[(p+1)!]^2} \prod_{j=0}^{p} (x - x_{i,j}) = R_{p+1,i},$$

since $L_{p+1,i}^{(p+1)} = \frac{2^{p+1}}{h_i^{p+1}} \tilde{L}_{p+1}^{(p+1)} = \frac{(2p+2)!}{h_i^{p+1}(p+1)!}$. Thus,

(20)
$$v - \pi v = d_{p+1} R_{p+1,i}(x).$$

On the other hand, since $P_h^- (L_{p+1,i}) \in P^p(I_i)$, it can be written as

(21)
$$P_h^- (L_{p+1,i}(x)) = \sum_{j=0}^{p} b_j L_{j,i}(x).$$

Multiplying (21) by $L_{k,i}(x)$, $k = 0, 1, \dots, p - 1$, integrating over I_i, using the orthogonality property of the projection P_h^-, and applying the relation (11f), we obtain, for $k = 0, 3, \dots, p - 1$,

$$0 = \int_{I_i} L_{k,i}(x) P_h^- (L_{p+1,i}(x)) dx = \sum_{j=0}^{p} b_j \int_{I_i} L_{k,i}(x) L_{j,i}(x) dx$$

$$= b_k \int_{I_i} L_{k,i}^2(x) dx$$

(22)
$$= b_k \frac{h_i}{2k+1}.$$

Consequently $b_k = 0$ for $k = 0, 1, \dots, p - 1$ so that

(23)
$$P_h^- (L_{p+1,i}(x)) = b_p L_{p,i}(x).$$

By the property of the projection P_h^-, $P_h^- v(x_i) = v(x_i)$, we have

(24)
$$1 = L_{p+1,i}(x_i) = P_h^- (L_{p+1,i}(x_i)) = b_p L_{p,i}(x_i) = b_p.$$

Thus, we get

(25)
$$P_h^- (L_{p+1,i}(x)) = L_{p,i}(x).$$

Combining (19) and (25), we obtain

(26)
$$v - P_h^- v = d_{p+1} \left(L_{p+1,i} - L_{p,i} \right) = d_{p+1} R_{p+1,i}.$$

From (20) and (26), we establish that

$$\pi v = P_h^- v, \quad \forall \, v \in P^{p+1}(I_i).$$

Next, we prove (16). Adding and subtracting $V = \hat{\pi}u = \sum_{k=0}^{p} a_k L_{k,i} + \alpha_i L_{p+1,i} \in P^{p+1}(I_i)$ we split the interpolation error as

$$u - \pi u = (u - V) + (V - \pi u) = \phi_i + \gamma_i,$$

where

$$\phi_i = V - \pi u, \quad \gamma_i = u - V = u - \hat{\pi}u.$$

We note that, by (14), $\pi u = \pi(\hat{\pi}u) = \pi V$. Thus, by (25), we get

$$
\begin{aligned}
\phi_i = V - \pi V &= \sum_{k=0}^{p} a_k L_{k,i} + \alpha_i L_{p+1,i} - \pi\left(\sum_{k=0}^{p} a_k L_{k,i} + \alpha_i L_{p+1,i}\right) \\
&= \alpha_i\left(L_{p+1,i} - \pi(L_{p+1,i})\right) \\
&= \alpha_i R_{p+1,i}.
\end{aligned}
$$

Multiplying $\hat{\pi}u = \sum_{k=0}^{p} a_k L_{k,i} + \alpha_i L_{p+1,i}$ by $L_{p+1,i}$, integrating over I_i, and using the orthogonality relation (11f), we obtain

$$\int_{I_i} L_{p+1,i}\hat{\pi}u \, dx = \sum_{k=0}^{p} a_k \int_{I_i} L_{p+1,i}L_{k,i}dx + \alpha_i \int_{I_i} L_{p+1,i}^2 dx = \alpha_i \frac{h_i}{2p+3},$$

which gives

$$\alpha_i = \frac{2p+3}{h_i}\int_{I_i} L_{p+1,i}\hat{\pi}udx.$$

Thus, we completed the proof of (16).

Next, we will prove (17). By the standard interpolation error estimates we have

$$(27) \qquad \|\phi_i\|_{k,I_i} \leq C_1 h_i^{p+1-k}\|V\|_{p+1,I_i}, \quad \|\gamma_i\|_{k,I_i} \leq C_2 h_i^{p+2-k}\|u\|_{p+2,I_i}.$$

Finally, we find a bound of $\|V\|_{p+1,I_i}$ by adding and subtracting u and applying the triangle inequality as

$$
\begin{aligned}
\|V\|_{p+1,I_i} \leq \|V - u\|_{p+1,I_i} + \|u\|_{p+1,I_i} &= \|\hat{\pi}u - u\|_{p+1,I_i} + \|u\|_{p+1,I_i} \\
&\leq (Ch_i + 1)\|u\|_{p+1,I_i} \\
&\leq C\|u\|_{p+1,I_i},
\end{aligned}
$$

which complete the proofs of (17).

In order to prove (18) we note that $\hat{\pi}u \in P^{p+1}(I_i)$, thus by (15) and (14), we have

$$(28) \qquad\qquad\qquad P_h^-\hat{\pi}u = \pi(\hat{\pi}u) = \pi u,$$

and by the standard interpolation error we have

$$(29) \qquad\qquad \|u - \hat{\pi}u\|_{0,I_i} \leq C_1 h_i^{p+2}\|u\|_{p+2,I_i}.$$

Applying P_h^- to $u = u - \hat{\pi}u + \hat{\pi}u$ and using (28), we obtain

$$P_h^-u = P_h^-(u - \hat{\pi}u) + P_h^-(\hat{\pi}u) = P_h^-(u - \hat{\pi}u) + \pi u,$$

which, in turn, yields

$$(30) \qquad P_h^- u - \pi u = P_h^- (u - \hat{\pi} u).$$

Now, we show that $\left\| P_h^- v \right\|_{0,I_i} \leq C_2 \left\| v \right\|_{0,I_i}$ by writing

$$
\begin{aligned}
\left\| P_h^- v \right\|_{0,I_i} = \left\| P_h^- v - v + v \right\|_{0,I_i} &\leq \left\| P_h^- v - v \right\|_{0,I_i} + \left\| v \right\|_{0,I_i} \\
&\leq C h_i^{p+1} \left\| v \right\|_{p+1,I_i} + \left\| v \right\|_{0,I_i} \\
(31) &\leq C_2 \left\| v \right\|_{0,I_i}.
\end{aligned}
$$

Taking the L^2 norm of (30) and applying the estimate (31) with $v = u - \hat{\pi} u$, we obtain

$$(32) \qquad \left\| P_h^- u - \pi u \right\|_{0,I_i} = \left\| P_h^- (u - \hat{\pi} u) \right\|_{0,I_i} \leq C_2 \left\| u - \hat{\pi} u \right\|_{0,I_i}.$$

Combining (32) and the standard interpolation estimates (29) we establish (18). $\qquad \square$

Now, we are ready to prove our main superconvergence result towards the right Radau interpolating polynomial. Furthermore, we show that the significant part of the discretization error for the LDG solution is proportional to the $(p+1)$-degree right Radau polynomial.

Theorem 3.1. *Under the assumptions of Theorem 2.1, there exists a constant C such that*

$$(33) \qquad \| u_h - \pi u \| \leq C h^{p + \frac{3}{2}},$$

and the actual error can be split as

$$(34a) \qquad e_u(x,t) = \alpha_i(t) R_{p+1,i}(x) + \omega_i(x,t), \quad \text{on } I_i,$$

where $\omega_i = \gamma_i + \pi u - u_h$, and

$$(34b) \qquad \sum_{i=1}^{N} \left\| \partial_x^k \omega_i \right\|_{0,I_i}^2 \leq C h^{2(p-k)+3}, \quad k = 0, 1, \quad \forall \, t \in [0, T].$$

Proof. Adding and subtracting $P_h^- u$ to $u_h - \pi u$, we have

$$u_h - \pi u = (u_h - P_h^- u) + (P_h^- u - \pi u) = -\bar{e}_u + P_h^- u - \pi u.$$

Taking the L^2-norm and using the triangle inequality, we get

$$\| u_h - \pi u \| \leq \| \bar{e}_u \| + \left\| P_h^- u - \pi u \right\|.$$

Using the estimates (10c) and (18), we establish (33).

Next, we add and subtract πu to e_u and we use (16) to obtain

$$(35) \qquad e_u = u - \pi u + \pi u - u_h = \phi_i + \gamma_i + \pi u - u_h = \phi_i + \omega_i,$$

where $\omega_i = \gamma_i + \pi u - u_h$.

Applying the Cauchy-Schwarz inequality and the inequality $ab \leq \frac{1}{2}(a^2 + b^2)$, we get

$$\|\omega_i\|_{0,I_i}^2 = \|\gamma_i\|_{0,I_i}^2 + 2 \int_{I_i} \gamma_i(\pi u - u_h)dx + \|\pi u - u_h\|_{0,I_i}^2$$
$$\leq 2\left(\|\gamma_i\|_{0,I_i}^2 + \|\pi u - u_h\|_{0,I_i}^2\right).$$

Summing over all elements and applying (17) and (33) yields

$$\sum_{i=1}^{N} \|\omega_i\|_{0,I_i}^2 \leq C_1 h^{2p+4} + C_2 h^{2p+3} \leq C h^{2p+3},$$

which completes the proof of (34b) for $k = 0$. Next, we use the Cauchy-Schwarz inequality and the inequality $ab \leq \frac{1}{2}(a^2 + b^2)$ to get

$$\|(\omega_i)_x\|_{0,I_i}^2 = \int_{I_i} \left((\gamma_i + \pi u - u_h)_x\right)^2 dx \leq 2\left(\|(\gamma_i)_x\|_{0,I_i}^2 + \|(\pi u - u_h)_x\|_{0,I_i}^2\right).$$

Using the inverse inequality $\|(\pi u - u_h)_x\|_{0,I_i} \leq Ch^{-1}\|\pi u - u_h\|_{0,I_i}$, we obtain the estimate

$$\|(\omega_i)_x\|_{0,I_i}^2 \leq C\left(\|(\gamma_i)_x\|_{0,I_i}^2 + h^{-2}\|\pi u - u_h\|_{0,I_i}^2\right).$$

Summing over all elements and applying (33) and the standard error estimate (17), we establish (34b) for $k = 1$.   □

Remark 3.2. *In Theorem 2.1, we proved that the LDG solution u_h converges to $P_h^- u$ at $\mathcal{O}(h^{p+\frac{3}{2}})$ rate while numerically the rate is observed of order $\mathcal{O}(h^{p+2})$. We used the estimate (10c) to prove that u_h converges to πu at $\mathcal{O}(h^{p+\frac{3}{2}})$ rate. We would like to point out that the superconvergence estimate of the error between u_h and $P_h^- u$ is not optimal. However, if one can prove the optimal estimate $\|u_h - P_h^- u\| = \mathcal{O}(h^{p+2})$, then the order of convergence of u_h to πu can be improved to be $\|u_h - \pi u\| = \mathcal{O}(h^{p+2})$ since, by (18), $\|P_h^- u - \pi u\| = \mathcal{O}(h^{p+2})$. It remains an open problem to investigate the optimal superconvergence estimates for this problem. In [28], the authors proved superconvergence results for the LDG method for the linear wave equation. Their theoretical analysis in not trivial to extend to the nonlinear case. In the linear case, it is easy to construct a correction function, which can be used to correct the error between the LDG solution and the Gauss-Radau projection of the exact solution $P_h^- u$. This problem is still open for the nonlinear case. Thus, proving optimal superconvergence results is still an open problem for the LDG method for nonlinear KdV equations.*

4. *A posteriori* error estimation

In this section, we construct a residual-based *a posteriori* error estimator for the LDG method for nonlinear KdV problems. The proposed estimator is obtained by solving a local steady problem with no boundary conditions

on each element. We further show that the LDG error estimate converges to the exact spatial error as $h \to 0$.

To obtain a procedure for computing the *a posteriori* error estimate, we replace u by $u_h + e_u$ and q by $q_h + e_q$ in the third equation of (2) *i.e.*, $q - u_x = 0$ to obtain

$$(36) \qquad (e_u)_x = q_h - (u_h)_x + e_q, \quad x \in I_i.$$

Multiplying (36) by a test function v and integrating over I_i, we get

$$(37) \qquad \int_{I_i} (e_u)_x v dx = \int_{I_i} (q_h - (u_h)_x + e_q) \, v dx.$$

Substituting (34a) into the left-hand side of (37) and choosing $v = L_{p,i}(x)$ yields

$$(38) \qquad \alpha_i \int_{I_i} R'_{p+1,i} L_{p,i} dx = \int_{I_i} (q_h - (u_h)_x + e_q - (\omega_i)_x) L_{p,i} dx.$$

Using (13), we obtain

$$(39) \qquad \alpha_i(t) = \frac{1}{2} \int_{I_i} (q_h - (u_h)_x + e_q - (\omega_i)_x) L_{p,i} dx.$$

Our error estimate procedure consists of approximating the true error e_u on each element I_i by the leading term as

$$(40) \qquad e_u(x,t) \approx E_u(x,t) = a_i(t) R_{p+1,i}(x), \quad x \in I_i,$$

where the coefficient of the leading term of the error at fixed time t, $a_i(t)$, is obtained from the coefficient $\alpha_i(t)$ defined in (39) by neglecting the terms ω_i and e_q, *i.e.*,

$$(41) \qquad a_i(t) = \frac{1}{2} \int_{I_i} (q_h - (u_h)_x) L_{p,i} dx.$$

The main results of this section are stated in the following theorem. In particular, we will show that the error estimate E_u converges to the true error e_u in the L^2-norm as $h \to 0$. Furthermore, we will prove the convergence to unity of the global effectivity index $\Theta_u(t)$ under mesh refinement.

Theorem 4.1. *Suppose that the assumptions of Theorem 2.1 are satisfied. If α_i and a_i are given by (39) and (41), respectively, and $E_u(x,t) = a_i(t) R_{p+1,i}(x)$, then there exists a constant C independent of h such that*

$$(42) \qquad \|e_u - E_u\| \leq C h^{p+\frac{3}{2}},$$

$$(43) \qquad |\|e_u\| - \|E_u\|| \leq C_1 h^{p+\frac{3}{2}}.$$

Finally, if there exists a constant $c = c(u) > 0$ independent of h with

$$(44) \qquad \|e_u\| \geq C h^{p+1},$$

then, at a fixed time t, the global effectivity index in the L^2 converges to unity at $\mathcal{O}(h^{\frac{1}{2}})$ rate i.e.,

$$(45) \qquad \Theta_u(t) = \frac{\|E_u\|}{\|e_u\|} = 1 + \mathcal{O}(h^{\frac{1}{2}}).$$

Proof. First, we will prove (42). Since $e_u = \alpha_i R_{p+1,i} + \omega_i$, and $E_u = a_i R_{p+1,i}$, we have

$$\|e_u - E_u\|_{0,I_i}^2 = \|(\alpha_i - a_i)R_{p+1,i} + \omega_i\|_{0,I_i}^2$$
$$\leq 2(\alpha_i - a_i)^2 \|R_{p+1,i}\|_{0,I_i}^2 + 2 \|\omega_i\|_{0,I_i}^2 \,,$$

where we used the inequality $(a+b)^2 \leq 2a^2 + 2b^2$. Summing over all elements and applying the estimate (34b) with $k = 0$ yields

$$\|e_u - E_u\|^2 = \sum_{i=1}^N \|e_u - E_u\|_{0,I_i}^2 \leq 2 \sum_{i=1}^N (\alpha_i - a_i)^2 \|R_{p+1,i}\|_{0,I_i}^2 + 2 \sum_{i=1}^N \|\omega_i\|_{0,I_i}^2$$

$$(46) \qquad\qquad\qquad \leq 2 \sum_{i=1}^N (\alpha_i - a_i)^2 \|R_{p+1,i}\|_{0,I_i}^2 + C_1 h^{2p+3}.$$

Next, we will estimate $\sum_{i=1}^N (\alpha_i - a_i)^2 \|R_{p+1,i}\|_{0,I_i}^2$. Subtracting (41) from (39) and applying the triangle inequality, we get

$$\left| \alpha_i - a_i \right| = \left| \frac{1}{2} \int_{I_i} (e_q - (\omega_i)_x) L_{p,i} dx \right| \leq \frac{1}{2} \int_{I_i} \left(|e_q| + |(\omega_i)_x| \right) |L_{p,i}| dx.$$

Using the inequality $(a + b)^2 \leq 2(a^2 + b^2)$ yields

$$(\alpha_i - a_i)^2 \leq \frac{1}{2} \left[\left(\int_{I_i} |e_q| |L_{p,i}| dx \right)^2 + \left(\int_{I_i} |(\omega_i)_x| |L_{p,i}| dx \right)^2 \right].$$

Applying the Cauchy-Schwarz inequality and the estimate (11f), we obtain

$$(\alpha_i - a_i)^2 \leq \frac{\|L_{p,i}\|_{0,I_i}^2}{2} \left(\|e_q\|_{0,I_i}^2 + \|(\omega_i)_x\|_{0,I_i}^2 \right)$$

$$(47) \qquad\qquad \leq \frac{h_i}{2(2p + 1)} \left(\|e_q\|_{0,I_i}^2 + \|(\omega_i)_x\|_{0,I_i}^2 \right).$$

Multiplying by $\|R_{p+1,i}\|_{0,I_i}^2$ and using (12) yields

$$(\alpha_i - a_i)^2 \|R_{p+1,i}\|_{0,I_i}^2 \quad \leq \quad \frac{h_i \|R_{p+1,i}\|_{0,I_i}^2}{2(2p + 1)} \left(\|e_q\|_{0,I_i}^2 + \|(\omega_i)_x\|_{0,I_i}^2 \right)$$

$$= \quad C_p h_i^2 \left(\|e_q\|_{0,I_i}^2 + \|(\omega_i)_x\|_{0,I_i}^2 \right),$$

where $C_p = \frac{c_p}{2(2p+1)} = \frac{2(p+1)}{(2p+1)^2(2p+3)}$ since $c_p = \frac{4(p+1)}{(2p+1)(2p+3)}$.

Finally, summing over all elements and using the fact that $h = \max\limits_{1 \leq i \leq N} h_i$, we conclude that

$$\sum_{i=1}^{N} (\alpha_i - a_i)^2 \|R_{p+1,i}\|_{0,I_i}^2 \leq C_p h^2 \left(\|e_q\|^2 + \sum_{i=1}^{N} \|(\omega_i)_x\|_{0,I_i}^2 \right).$$

Applying the estimates (10a) and (34b) with $k = 1$, we establish

$$(48) \quad \sum_{i=1}^{N} (\alpha_i - a_i)^2 \|R_{p+1,i}\|_{0,I_i}^2 \leq C_p h^2 (C_1 h^{2p+2} + C_2 h^{2p+1}) \leq C h^{2p+3}.$$

Now, combining (46) with (48) yields

$$\|e_u - E_u\|^2 \leq C_1 h^{2p+3} + C_2 h^{2p+3} \leq C h^{2p+3},$$

which completes the proof of (42).

In order to prove (43), we use the reverse triangle inequality to have

$$(49) \quad \big| \|E_u\| - \|e_u\| \big| \leq \|E_u - e_u\|.$$

Combining (49) and (42) completes the proof of (43).

In order to prove (45), we divide the inequality in (49) by $\|e_u\|$ and we use the estimate (42) and the assumption (44) to obtain

$$\left| \frac{\|E_u\|}{\|e_u\|} - 1 \right| \leq \frac{\|E_u - e_u\|}{\|e_u\|} \leq \frac{C_1 h^{p+\frac{3}{2}}}{C h^{p+1}} \leq C h^{\frac{1}{2}}.$$

Therefore, $\frac{\|E_u\|}{\|e_u\|} = 1 + \mathcal{O}(h^{\frac{1}{2}})$, which completes the proof of (45). $\qquad\square$

In the previous theorem, we proved that the residual-based *a posteriori* error estimate E_u converges to the true spatial error e_u in the L^2-norm at $\mathcal{O}(h^{p+\frac{3}{2}})$ rate. We also proved that the global effectivity index in the L^2-norm converges to unity at $\mathcal{O}(h^{\frac{1}{2}})$ rate. We note that E_u is a computable quantity since it only depends on the LDG solutions u_h and q_h. Additionally, (45) indicates that the computable quantity $\|E_u\|$ provides an asymptotically exact *a posteriori* estimator on the actual error $\|e_u\|$. We remark that $\|E_u\|$ is computationally efficient since

$$\|E_u\|^2 = \sum_{i=1}^{N} \|E_u\|_{0,I_i}^2 = \sum_{i=1}^{N} |a_i| \|R_{p+1,i}\|_{0,I_i}^2 = c_p \sum_{i=1}^{N} |a_i| h_i,$$

where $c_p = \frac{4(p+1)}{(2p+1)(2p+3)}$ and a_i is given by (41). Finally, we would like to mention that the computable quantity $u_h + E_u$ converges to the exact solution u at $\mathcal{O}(h^{p+\frac{3}{2}})$ rate since

$$\|u - (u_h + E_u)\| = \|e_u - E_u\| \leq C h^{p+\frac{3}{2}}.$$

We emphasize that this accuracy enhancement is achieved by adding the error estimate E_u to the LDG solution u_h only once at the end of the computation *i.e.*, at $t = T$.

An accepted efficiency measure of *a posteriori* error estimate is the effectivity index. In this paper, we use the global effectivity index $\Theta_u(t) = \frac{\|E_u\|}{\|e_u\|}$. Ideally, the global effectivity index should stay close to one and should converge to one under mesh refinement.

Remark 4.1. *The assumption in (44) imply that the term of order $\mathcal{O}(h^{p+1})$ is present in the error e_u. Even though the proof of (45) is valid under the assumption (44), our computational results given in the next section suggest that the global effectivity index Θ_u in the L^2-norm converges to unity with at least $\mathcal{O}(h)$ rate. Thus, the proposed* a posteriori *error estimation technique is an excellent measure of the error and (45) indicates that our* a posteriori *error estimator is asymptotically exact.*

5. Numerical examples

In this section, we numerically validate our superconvergence results and the global convergence of the proposed residual-based *a posteriori* error estimates. The initial condition is determined by $u_h(x,0) = \mathbb{P}_h u(x,0)$. We also used $u_h(x,0) = P_h^- u(x,0)$ and observed similar results. Temporal integration is performed by the fourth-order Runge-Kutta method. A time step Δt is chosen so that temporal errors are small relative to spatial errors. We do not discuss the effect of the time discretization error in this paper.
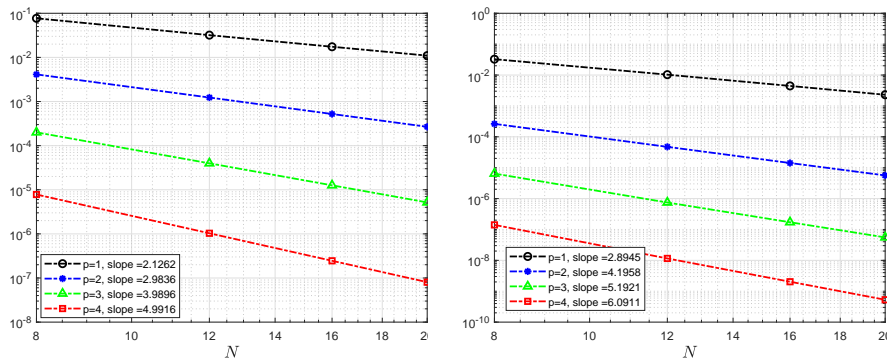
FIGURE 1. Log-log plots of $\|u - u_h\|$ (left) and $\|u_h - \pi u\|$ (right) versus mesh sizes h for Example 5.1 on uniform meshes having $N = 8$, 12, 16, 20 elements using P^p, $p = 1, 2, 3, 4$.

Example 5.1. In this example, we apply the LDG method to the following nonlinear KdV problem subject to the periodic boundary condition

$$(50) \quad \begin{cases} u_t + (u^3 + u)_x + u_{xxx} = g(x,t), \ x \in [0, 2\pi], \ t \in [0,1], \\ u(x,0) = \sin(x), \quad x \in [0, 2\pi]. \end{cases}$$
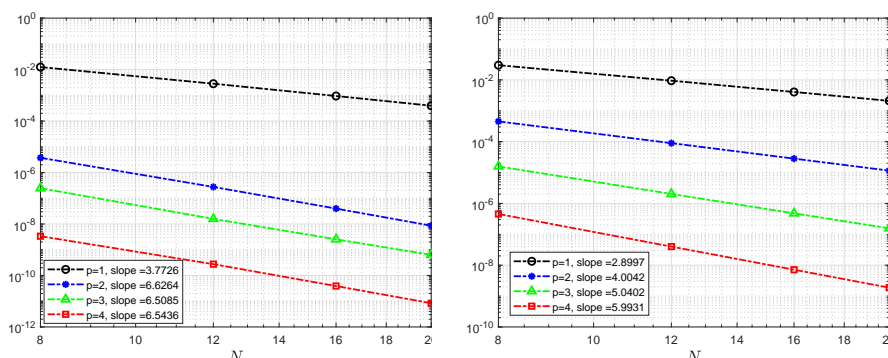
FIGURE 2. Log-log plots of $\big|\,\|e_u\| - \|E_u\|\,\big|$ (left) and $\|e_u - E_u\|$ (right) versus mesh sizes h for Example 5.1 on uniform meshes having $N = 8, 12, 16, 20$ elements using P^p, $p = 1, 2, 3, 4$.

We select the source term $g(x,t)$ such that the exact solution is $u(x,t) = \sin(x+t)$. We note that $f'(u) = 3u^2 + 1 > 0$ so the numerical flux $\hat{f}$ is simply the upwind flux $\hat{f}\big|_i = f(u_h^-)\big|_i$. We solve (50) using the LDG method on uniform meshes obtained by partitioning the computational domain $[0, 2\pi]$ into N subintervals with $N = 8, 12, 16, 20$ and using the finite element spaces P^p with $p = 1, 2, 3, 4$. Figure 1 shows the actual L^2 errors $\|e_u\| = \|u - u_h\|$ and the L^2 errors between the LDG solution u_h and the p-degree interpolating right Radau polynomial πu at $t = 1$ with log-log scale as well as their orders of convergence. The L^2 errors are presented in log scale just for easy visualization. For each P^p space, we fit, in a least-squares sense, the data sets with a linear function and then determine from the fitting result the slopes of the fitting lines. The slopes of the fitting lines are shown on the graph for $p = 1, 2, 3, 4$. These results indicate that $\|u - u_h\|$ converges at $\mathcal{O}(h^{p+1})$ rate whereas $\|u_h - \pi u\|$ converges at $\mathcal{O}(h^{p+2})$ rate. Thus, the LDG solution u_h is superconvergent with order $p+2$ to the p-degree interpolating right Radau polynomial πu. Although the superconvergence rate is proved to be of order $p + \frac{3}{2}$, our computational results indicate that the observed numerical convergence rate is higher than the theoretical rate. In Figure 2 we present the global errors $\big|\,\|e_u\| - \|E_u\|\,\big|$ and $\|e_u - E_u\|$ at $t = 1$. These results indicate that $\big|\,\|e_u\| - \|E_u\|\,\big| = \mathcal{O}(h^{p+2.5})$ and $\|e_u - E_u\| = \mathcal{O}(h^{p+2})$. We note that the observed numerical convergence rates are higher than the theoretical rates established in Theorem 4.1. The results shown in Table 1 indicate that the global effectivity indices converge to unity under h-refinement. The numerical convergence rates at $t = 1$ for $\big|\Theta_u - 1\big|$ are also shown in Table 1, which suggest that the convergence rate is higher than the theoretical rate established in Theorem 4.1. The global effectivity index $\Theta_u(t)$, $t \in [0, 1]$ is

shown in Figures 3 and 4 using $(p, N) = (3, 12), (4, 12), (3, 20), (4, 20)$. We observe that the effectivity index remains constant as we refine the mesh.
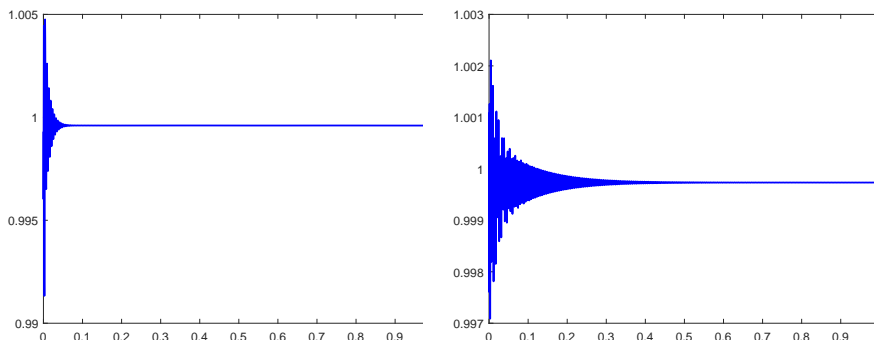
FIGURE 3. Global effectivity index $\Theta_u(t)$, $t \in [0, 1]$ versus time for Example 5.1 using $(p, N) = (3, 12)$ (left) and $(p, N) = (4, 12)$ (right).
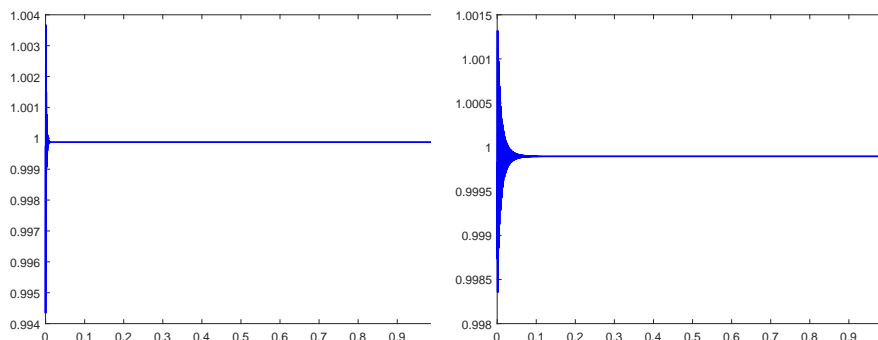
FIGURE 4. Global effectivity index $\Theta_u(t)$, $t \in [0, 1]$ versus time for Example 5.1 using $(p, N) = (3, 20)$ (left) and $(p, N) = (4, 20)$ (right).

Example 5.2. In this example, we consider the following nonlinear KdV equation

$$(51) \qquad \begin{cases} u_t + (3u^2)_x + u_{xxx} = g(x, t), \ x \in [0, 2\pi], \ t \in [0, 1], \\ u(x, 0) = \sin(x), \quad x \in [0, 2\pi]. \end{cases}$$

with periodic boundary conditions. Here, g is chosen so that the exact solution is $u(x, t) = \sin(x + t)$ on the domain $(x, t) \in [0, 2\pi] \times [0, 1]$. We note that $f'(u) = u$ changes sign in the computational domain. In this case, we use the Godunov flux (4d). We solve this problem using the LDG method on uniform meshes having $N = 8, 12, 16, 20$ elements and using P^p polynomials with $p = 1, 2, 3, 4$. The L^2 LDG errors $\|u - u_h\|$ and

TABLE 1. Θ_u and the errors $\left|\Theta_u - 1\right|$ with their orders of convergence at $t = 1$ for Example 5.1 on uniform meshes having $N = 4, 8, 12, 16, 20$ elements using P^p, $p = 1, 2, 3, 4$.

N	$p = 1$			$p = 2$		
	Θ_u	$\left\|\Theta_u - 1\right\|$	Order	Θ_u	$\left\|\Theta_u - 1\right\|$	Order
4	0.70236	2.9764e-01	–	0.95223	4.7774e-02	–
8	0.83708	1.6292e-01	0.8694	0.99909	9.0992e-04	5.7143
12	0.91148	8.8519e-02	1.5045	0.99978	2.2393e-04	3.4578
16	0.94601	5.3987e-02	1.7188	0.99992	7.6255e-05	3.7446
20	0.96407	3.5930e-02	1.8247	0.99997	3.2214e-05	3.8616
N	$p = 3$			$p = 4$		
	Θ_u	$\left\|\Theta_u - 1\right\|$	Order	Θ_u	$\left\|\Theta_u - 1\right\|$	Order
4	0.96977	3.0235e-02	–	0.99854	1.4566e-03	–
8	0.99877	1.2302e-03	4.6193	0.99957	4.3036e-04	1.759
12	0.99960	3.9834e-04	2.7811	0.99973	2.6642e-04	1.1827
16	0.99980	2.0163e-04	2.3668	0.99984	1.5837e-04	1.808
20	0.99988	1.2276e-04	2.2237	0.99990	1.0388e-04	1.8898

$\|u_h - \pi u\|$ at time $t = 1$ shown in Figure 5. As before, we observe that $\|u - u_h\| = \mathcal{O}(h^{p+1})$ but $\|u_h - \pi u\| = \mathcal{O}(h^{p+2})$. Consequently, the LDG solution u_h is superconvergent with order $p+2$ to the p-degree interpolating right Radau polynomial πu. Again the computational results indicate that the numerical convergence rate is higher than the theoretical rate, which is proved to be of order $p + \frac{3}{2}$. In Figure 6 we present the errors $\left|\,\|e_u\| - \|E_u\|\,\right|$, $\|e_u - E_u\|$, and their order of convergence at $t = 1$. Clearly both errors converge with order higher than the theoretical rate, which is proved to be $p + \frac{3}{2}$ under mesh refinement. Table 2 lists the global effectivity indices and the errors $\left|\Theta_u - 1\right|$ with their order of convergence at $t = 1$. These results indicate that the proposed *a posteriori* LDG error estimate is asymptotically exact under mesh refinement. The convergence rate at $t = 1$ for $\left|\Theta_u - 1\right|$ is higher than $\mathcal{O}(h)$. Even though the assumption $f'(u) \geq 0$ does not always hold true, the same results are observed.

Example 5.3. In this example, we consider the following nonlinear KdV equation with flux function $f(u) = e^u$

(52)
$$\begin{cases} u_t + (e^u)_x + u_{xxx} = g(x,t), & x \in [0, 2\pi], \ t \in [0, 1], \\ u(x, 0) = \sin(x), & x \in [0, 2\pi]. \end{cases}$$

with periodic boundary conditions. We select g so that the exact solution is $u(x, t) = \sin(x + t)$ on the domain $(x, t) \in [0, 2\pi] \times [0, 1]$. We solve this problem using the LDG method on uniform meshes having $N = 8, 12, 16, 20, 24$ elements and using P^p polynomials with $p = 1, 2, 3$. In Figure 7 we
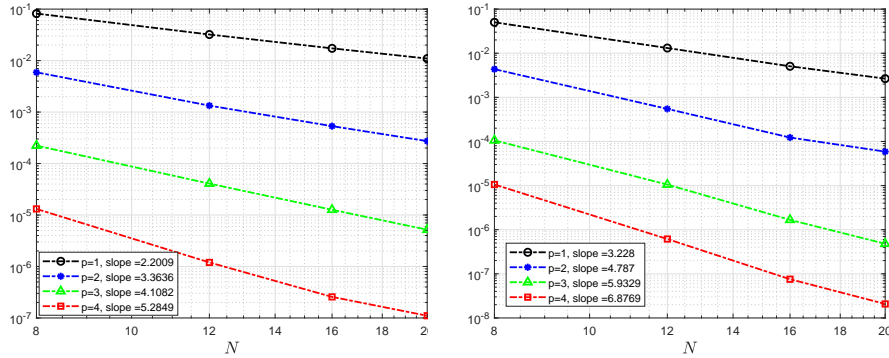
FIGURE 5. Log-log plots of $\|u - u_h\|$ (left) and $\|u_h - \pi u\|$ (right) versus mesh sizes h for Example 5.2 on uniform meshes having $N = 8$, 12, 16, 20 elements using P^p, $p = 1$, 2, 3, 4.
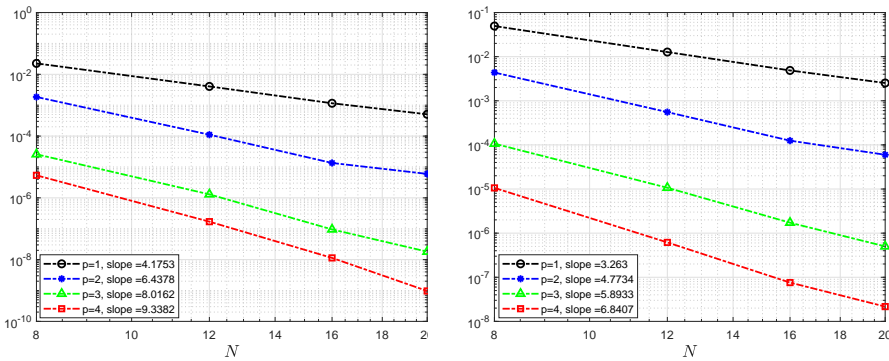
FIGURE 6. Log-log plots of $\big|\|e_u\| - \|E_u\|\big|$ (left) and $\|e_u - E_u\|$ (right) versus mesh sizes h for Example 5.2 on uniform meshes having $N = 8$, 12, 16, 20 elements using P^p, $p = 1$, 2, 3, 4.

report the L^2 LDG errors $\|u - u_h\|$ and $\|u_h - \pi u\|$ at time $t = 1$. Again, we observe that $\|u - u_h\| = \mathcal{O}(h^{p+1})$ and $\|u_h - \pi u\| = \mathcal{O}(h^{p+2})$. Thus, the LDG solution u_h is superconvergent with order $p + 2$ to the p-degree interpolating right Radau polynomial πu. In Figure 8 we present the errors $\big|\|e_u\| - \|E_u\|\big|$, $\|e_u - E_u\|$, and their order of convergence at $t = 1$. We observe that these errors converge with order higher than the theoretical rate, which is proved to be $p + \frac{3}{2}$ under mesh refinement.

TABLE 2. Θ_u and the errors $\left|\Theta_u - 1\right|$ with their orders of convergence at $t = 1$ for Example 5.2 on uniform meshes having $N = 4, 8, 12, 16, 20$ elements using P^p, $p = 1, 2, 3, 4$.

N	$p = 1$			$p = 2$		
	Θ_u	$\left|\Theta_u - 1\right|$	Order	Θ_u	$\left|\Theta_u - 1\right|$	Order
4	0.36379	6.3621e-01	–	0.33641	6.6359e-01	–
8	0.72464	2.7536e-01	1.2082	0.68769	3.1231e-01	1.0873
12	0.87373	1.2627e-01	1.9229	0.91684	8.3160e-02	3.2635
16	0.93320	6.6801e-02	2.2132	0.97471	2.5290e-02	4.1378
20	0.95367	4.6333e-02	1.6396	0.97814	2.1859e-02	0.65337
N	$p = 3$			$p = 4$		
	Θ_u	$\left|\Theta_u - 1\right|$	Order	Θ_u	$\left|\Theta_u - 1\right|$	Order
4	0.23828	7.6172e-01	–	0.29851	7.0149e-01	–
8	0.88436	1.1564e-01	2.7196	0.59125	4.0875e-01	0.7792
12	0.96815	3.1849e-02	3.1802	0.85875	1.4125e-01	2.6206
16	0.99249	7.5059e-03	5.0240	0.95571	4.4286e-02	4.0318
20	0.99650	3.4971e-03	3.4227	0.98343	1.6565e-02	4.4069
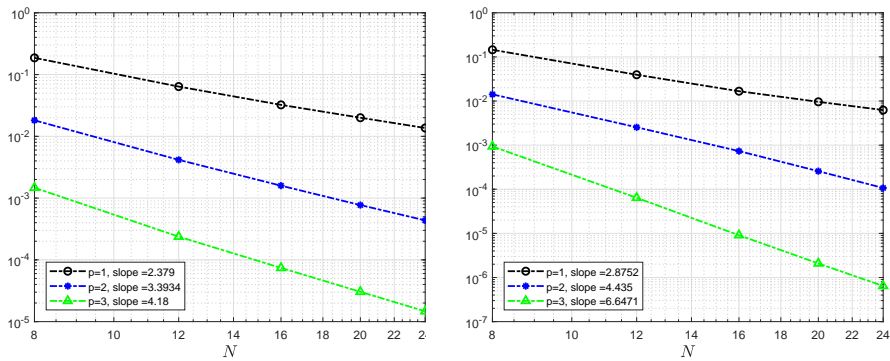
FIGURE 7. Log-log plots of $\|u - u_h\|$ (left) and $\|u_h - \pi u\|$ (right) versus mesh sizes h for Example 5.3 on uniform meshes having $N = 8, 12, 16, 20, 24$ elements using P^p, $p = 1, 2, 3, 4$.

6. Concluding remarks

In this paper, we proposed and analyzed *a posteriori* error estimator for the LDG method applied to nonlinear third-order KdV equations. We proved that the significant part of the discretization error for the p-degree LDG solution is proportional to a $(p + 1)$-degree right Radau polynomial.
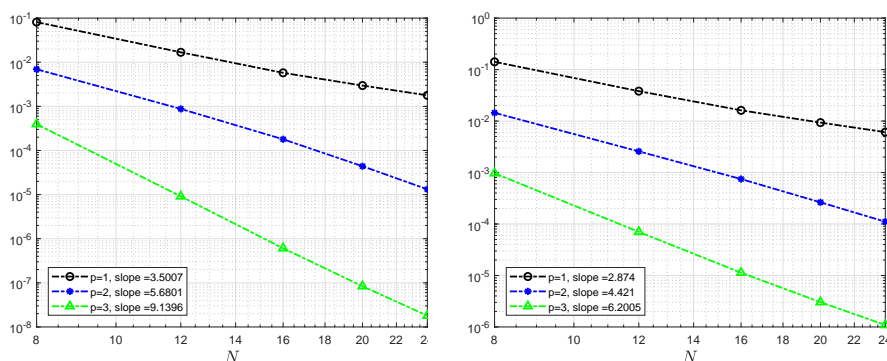
FIGURE 8. Log-log plots of $\big|\,\|e_u\| - \|E_u\|\,\big|$ (left) and $\|e_u - E_u\|$ (right) versus mesh sizes h for Example 5.3 on uniform meshes having $N = 8$, 12, 16, 20, 24 elements using P^p, $p = 1$, 2, 3, 4.

We used these results to construct asymptotically exact *a posteriori* error estimates. The *a posteriori* error estimator is computationally simple, efficient, and asymptotically exact. This estimator is obtained by solving a local residual problem on each element. The proposed *a posteriori* error estimate is shown to converge to the actual error in the L^2-norm under mesh refinement. The order of convergence is proved to be $p + \frac{3}{2}$, when piecewise polynomials of degree $p \geq 1$ are used. Our numerical experiments demonstrate that the results in this paper hold true for nonlinear problems with general flux functions, indicating that the restriction on $f(u)$ is artificial. The generalization of our proofs to nonlinear equations with general flux functions involves several technical difficulties and will be investigated in the future. We are currently investigating the superconvergence properties and the asymptotic exactness of *a posteriori* error estimates for LDG methods applied to two-dimensional KdV problems and wave equations on rectangular and triangular meshes. Our future work will focus on extending our *a posteriori* error analysis to problems on tetrahedral meshes. Also, because we observed superconvergence of order $p + 2$ in our numerical examples, future work will include investigating how to improve our proofs to obtain optimal superconvergence results. We expect that a similar special projection of the initial conditions of Yang and Shu [39] and a new technique will be needed to obtain the optimal rate of superconvergence.

Conflict of Interest: The author declares that he has no conflict of interest.

References

[1] M. Abramowitz, I. A. Stegun, Handbook of Mathematical Functions, Dover, New York, 1965.

[2] S. Adjerid, M. Baccouch, A superconvergent local discontinuous Galerkin method for elliptic problems, Journal of Scientific Computing 52 (2012) 113–152.

[3] M. Baccouch, A local discontinuous Galerkin method for the second-order wave equation, Computer Methods in Applied Mechanics and Engineering 209–212 (2012) 129–143.

[4] M. Baccouch, Asymptotically exact *a posteriori* LDG error estimates for one-dimensional transient convection-diffusion problems, Applied Mathematics and Computation 226 (2014) 455 – 483.

[5] M. Baccouch, The local discontinuous Galerkin method for the fourth-order Euler-Bernoulli partial differential equation in one space dimension. Part I: Superconvergence error analysis, Journal of Scientific Computing 59 (2014) 795–840.

[6] M. Baccouch, The local discontinuous Galerkin method for the fourth-order Euler-Bernoulli partial differential equation in one space dimension. Part II: *A posteriori* error estimation, Journal of Scientific Computing 60 (2014) 1–34.

[7] M. Baccouch, Superconvergence and *a posteriori* error estimates for the LDG method for convection-diffusion problems in one space dimension, Computers & Mathematics with Applications 67 (2014) 1130–1153.

[8] M. Baccouch, Superconvergence and *a posteriori* error estimates of a local discontinuous Galerkin method for the fourth-order initial-boundary value problems arising in beam theory, International journal of numerical analysis and modeling, series B 5 (2014) 188–216.

[9] M. Baccouch, Superconvergence of the local discontinuous Galerkin method applied to the one-dimensional second-order wave equation, Numerical methods for partial differential equations 30 (2014) 862–901.

[10] M. Baccouch, A superconvergent local discontinuous Galerkin method for the second-order wave equation on Cartesian grids, Computers and Mathematics with Applications 68 (2014) 1250–1278.

[11] M. Baccouch, Asymptotically exact *a posteriori* local discontinuous Galerkin error estimates for the one-dimensional second-order wave equation, Numerical methods for partial differential equations 31 (2015) 1461–1491.

[12] M. Baccouch, Asymptotically exact local discontinuous Galerkin error estimates for the linearized Korteweg-de Vries equation in one space dimension, International Journal of Numerical Analysis and Modeling 12 (2015) 162–195.

[13] M. Baccouch, Optimal *a Posteriori* error estimates of the local discontinuous Galerkin method for convection-diffusion problems in one space dimension, Journal of Computational Mathematics 34 (2016) 511–531.

[14] M. Baccouch, An optimal *a posteriori* error estimates of the local discontinuous Galerkin method for the second-order wave equation in one space dimension, International Journal of Numerical Analysis and Modeling 14 (2017) 355–380.

[15] M. Baccouch, Optimal energy-conserving local discontinuous Galerkin method for the one-dimensional sine-Gordon equation, International Journal of Computer Mathematics 94 (2017) 316–344.

[16] M. Baccouch, Superconvergence of the local discontinuous Galerkin method for the sine-Gordon equation on Cartesian grids, Applied Numerical Mathematics 113 (2017) 124 – 155.

[17] M. Baccouch, *A posteriori* local discontinuous Galerkin error estimates for the one-dimensional sine-Gordon equation, International Journal of Computer Mathematics 95 (4) (2018) 815–844.

[18] M. Baccouch, Superconvergence of the local discontinuous Galerkin method for the sine-Gordon equation in one space dimension, Journal of Computational and Applied Mathematics 333 (2018) 292 – 313.

[19] M. Baccouch, Superconvergence of the semi-discrete local discontinuous Galerkin method for nonlinear KdV-type problems, Discrete and Continuous Dynamical System - B 22 (2018) 1–36.

[20] M. Baccouch, A superconvergent local discontinuous Galerkin method for nonlinear two-point boundary-value problems, Numerical Algorithms 79 (3) (2018) 697–718.

[21] M. Baccouch, An adaptive local discontinuous Galerkin method for nonlinear two-point boundary-value problems, Numerical Algorithms (2019) 1–33.

[22] M. Baccouch, Analysis of optimal superconvergence of a local discontinuous Galerkin method for nonlinear second-order two-point boundary-value problems, Applied Numerical Mathematics 145 (2019) 361 – 383.

[23] M. Baccouch, A superconvergent local discontinuous Galerkin method for nonlinear fourth-order boundary-value problems, International Journal of Computational Methods 5 (56) (2019) 1950035.

[24] M. Baccouch, Analysis of optimal superconvergence of the local discontinuous Galerkin method for nonlinear fourth-order boundary value problems, Numerical Algorithms (2020) doi=10.1007/s11075–020–00947–0.

[25] M. Baccouch, *A posteriori* error analysis of the local discontinuous Galerkin method for the sine-Gordon equation in one space dimension, Journal of Computational and Applied Mathematics 366 (2020) 112432.

[26] M. Baccouch, S. Adjerid, *A posteriori* local discontinuous Galerkin error estimation for two-dimensional convection-diffusion problems, Journal of Scientific Computing 62 (2014) 399–430.

[27] T. Benjamin, J. Bona, J. Mahony, Model Equations for Long Waves in Nonlinear Dispersive Systems, Philosophical transactions A, Royal Society, 1972.

[28] W. Cao, D. Li, Z. Zhang, Optimal superconvergence of energy conserving local discontinuous Galerkin methods for wave equations, Communications in Computational Physics 21 (1) (2017) 211–236.

[29] B. Cockburn, C. W. Shu, The local discontinuous Galerkin method for time-dependent convection-diffusion systems, SIAM Journal on Numerical Analysis 35 (1998) 2440–2463.

[30] T. Dauxois, M. Peyrard, Physics of Solitons, Cambridge University Press, 2006.

[31] C. Hufford, Y. Xing, Superconvergence of the local discontinuous Galerkin method for the linearized Korteweg-de Vries equation, Journal of Computational and Applied Mathematics 255 (2014) 441–455.

[32] C.-W. Shu, Discontinuous Galerkin method for time-dependent problems: Survey and recent developments, in: X. Feng, O. Karakashian, Y. Xing (eds.), Recent Developments in Discontinuous Galerkin Finite Element Methods for Partial Differential Equations, vol. 157 of The IMA Volumes in Mathematics and its Applications, Springer International Publishing, 2014, pp. 25–62.

[33] Y. Xu, C.-W. Shu, Local discontinuous Galerkin methods for two classes of two dimensional nonlinear wave equations, Physica D 208 (2005) 21–58.

[34] Y. Xu, C.-W. Shu, Error estimates of the semi-discrete local discontinuous Galerkin method for nonlinear convection-diffusion and KdV equations, Computer Methods in Applied Mechanics and Engineering 196 (2007) 3805–3822.

[35] Y. Xu, C.-W. Shu, Local discontinuous Galerkin methods for high-order time-dependent partial differential equations, Communications in Computational Physics 7 (2010) 1–46.

[36] Y. Xu, C.-W. Shu, Optimal error estimates of the semi-discrete local discontinuous Galerkin methods for high order wave equations, SIAM Journal on Numerical Analysis 50 (2012) 79–104.

[37] J. Yan, C.-W. Shu, A local discontinuous Galerkin method for KdV type equations, SIAM Journal on Numerical Analysis 40 (2002) 769–791.

[38] J. Yan, C.-W. Shu, Local discontinuous Galerkin methods for partial differential equations with higher order derivatives, Journal of Scientific Computing 17 (2002) 27–47.

[39] Y. Yang, C.-W. Shu, Analysis of optimal superconvergence of discontinuous Galerkin method for linear hyperbolic equations, SIAM Journal on Numerical Analysis 50 (2012) 3110–3133.

Department of Mathematics, University of Nebraska at Omaha, Omaha, NE 68182, USA

E-mail: `mbaccouch@unomaha.edu`